Chapter 1

NONLINEAR PHENOMENA IN METALLIC CONTACTS

I. O. Kulik
Department of Physics, Bilkent University
Ankara 06533, Turkey

Abstract   We review and extend theoretical approaches to nonlinear and nonequilibrium effects in metallic microcontacts ranging in their dimension from the atomic to macroscopic sizes. *Atomic* contacts are shown to quantize their conductance in units of $2e^2/h$ provided the charge redistributes near the constriction to establish the maximal electron transmittivity through the orifice. *Ballistic* semiclassical contacts are treated both from the Landauer point of view and from the Boltzmann transport theory. The *J-V* nonlinearity in contacts is related to the inelastic scattering near the narrowest part of the constriction and permits for spectroscopic investigation of phonons in solids (the point-contact spectroscopy).The effects of phonon emission and reabsorption in contacts are taken into consideration. Phonon relaxation is shown to determine the frequency dependence of the nonlinear contact conductivity. *Thermal* contacts develop specific nonequilibrium states with *hot spots* in the center of metallic constriction whose temperature is much in excess of the ambient contact temperature and is uniquely related to voltage.

1. INTRODUCTION

It is the aim of this paper to present a coherent approach to linear and nonlinear, as well as to equilibrium and nonequilibrium, phenomena in metallic contacts of diameter ranging from the atomic size to macroscopic size. Our understanding of these properties arises from the works of Landauer [1], Sharvin [2], Yanson [3], Holland groups [4, 5], and others [6], *etc.* Unlike tunneling junctions, direct metallic constrictions (or links) develop a number of peculiarities of which we mention the following.

(1) Conductance of contact scales with the quantum of conductance

$$G_0 = \frac{2e^2}{h} = 1/12.9\text{k}\Omega \tag{1.1}$$

in such a way that minimal conductance reaches a value G_0 before the contact breaks to the tunneling-type junction with a much smaller or zero conductance, and is even quantized in units of $G_0 = R_0^{-1}$ in a proper arrangement. In particular, this happens if contact size or shape is varied by applying a gate voltage to change the electron concentration (in semiconducting constrictions), or contacting electrodes are pulled away to increase the length (and possibly the contacting area), in metallic contacts. The typical dependence of the contact conductance on the pulling strength [7] is presented in Fig. 1.1.
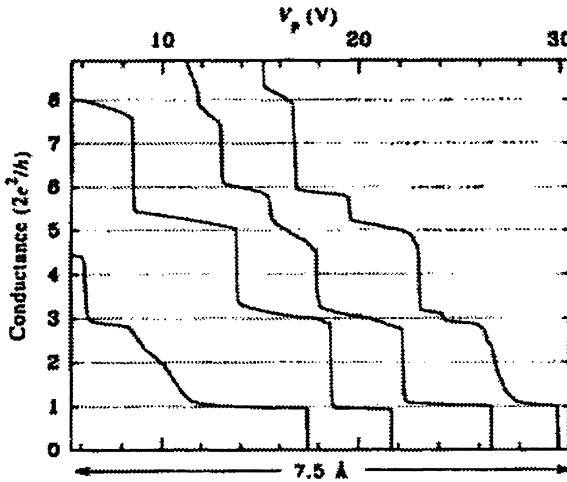

Figure 1.1 Conductance of sodium contact at 4.2 K as a function of stretch [7]. Measurements have been performed by pressing two pieces of metal and then pulling them away from one another with a piezoelectric sensor. Reproduced by permission from Ref. [7].

(2) The electron flow in a constriction is a regular quantum process (a kind of "nondemolition measurement") while the energy dissipation takes place away from its narrowest part. Because of this, the shot noise in direct metallic constriction reduces compared to its value in the tunneling junction of similar resistance [8]

$$S_V \sim 2eVR\frac{d}{l} \tag{1.2}$$

where S_V is the shot noise power and l the phase-breaking electron mean free path assumed to be larger than the contact diameter d. Reduced

shot noise in a metallic contacts was first observed in an experiment in 1984 [9] (see Fig. 1.2). (Further works are reviewed in [10].)
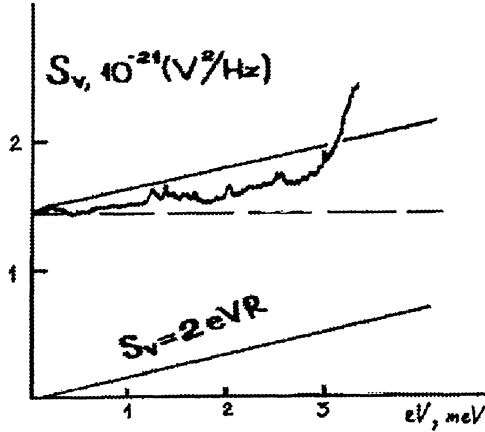

Figure 1.2 Current noise in a Na microcontact at $T = 1.7$ K [9]. Contact was produced by shortening a tunneling barrier between two metallic electrodes with an electric shock creating a small metallic bridge between the electrodes. Taken from Ref. [9].

(3) The superconducting properties of contacts with direct metallic conductivity are controlled by the Andreev reflection [11]. In short narrow constrictions ($d \ll \xi$ where ξ is a superconducting coherence length), the current-phase relation is nonsinusoidal [12]

$$J(\varphi) = G\frac{\pi\Delta}{e}\sin\frac{\varphi}{2}\tanh\frac{\Delta\cos\frac{\varphi}{2}}{2T} \qquad (1.3)$$

unlike in the tunneling Josephson junctions, and larger in magnitude than the critical Josephson current at same conductance.

(4) Nonlinearity in the contact conductance arises due to inelastic processes of electron-phonon interaction (EPI) in the narrowest part of constriction where the drift velocity of electrons approaches the velocity of acoustic waves. The derivative of current with respect to voltage is proportional to the density of phonon states (and also to the frequency dependent matrix element of EPI)

$$\frac{dG}{dV}(V) \simeq F(\omega)|_{\omega=eV/\hbar} \qquad (1.4)$$

thus providing for the spectroscopy of phonons with microcontacts [3, 4]. An example of the nonlinear current-voltage characteristics of microcontact [14] is shown in Fig. 1.3. Metallic contacts survive quite large voltage biases (say, $eV \sim 100$ mV) at which a small region of metal near the

orifice enters into the extreme nonequilibrium, nonthermal state super-
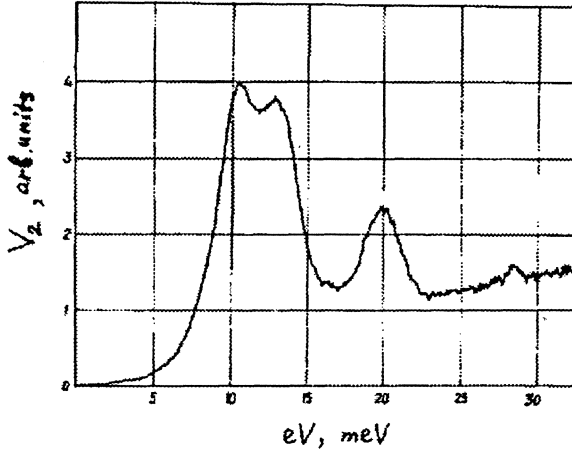imposed over the background of the cold lattice.

Figure 1.3 Point-contact spectrum of EPI in *Ag* needle-anvil contact at 1.6 K [14].
Second derivative of the $J - V$ characteristics was recorded by measuring the ampli-
tude of the second harmonic, V_2, of the oscillating voltage versus the *d.c.* voltage on
the contact, V. Taken from Ref. [28].

(5) In plastically deformed contacts, phonons emitted due to electron
scattering reabsorb near the orifice. Since phonon relaxation rate is much
slower than the electron relaxation, the nonlinear electron conductivity
shows a dispersion at characteristics frequencies [15, 16]

$$\nu_{ph} \simeq \lambda \frac{s}{v_F} \omega_D \sim 10^{10} \text{ s}^{-1} \tag{1.5}$$

(6) Larger-size contacts, $d \geq 100$ nm, enter the non-ballistic regime
of current transport in which **hot spot** is formed near the orifice with a
high temperature uniquely related to voltage [17]

$$k_B T = 3.63 eV \tag{1.6}$$

resulting in a strong nonlinearity of its $J(V)$ dependence and the tran-
sistor effect [18].

The theoretical description of contacts divide them into three cate-
gories:

- *Atomic* contacts with the size of the order of few atoms. The
  mechanism of conduction is described as hopping between atomic
  sites similar to tight-binding approximation in the theory of solids.

- *Ballistic* microcontacts, those of size larger than the atomic size but smaller than the mean free path of electrons

$$a \ll d \ll l \qquad\qquad (1.7)$$

Such contacts are treated in a semiclassical approximation using transport theories such as the Boltzmann kinetic equations.

- *Thermal* contacts $(d \gg l)$ developing, due to a current concentration, "hot spots" of small size in a very cold steady state environment.

2. ATOMIC CONTACTS

The model of contact [19] assumes regular arrangement of atoms in its narrowest part in the form of two cone-shaped surfaces contacting over a plate with N_t atoms (and possibly making a bridge of length of L atoms), and connected through N_l leads to the thermal reservoirs specified with their respective temperatures (T_i), voltages (V_i) and phases of the order parameter (φ_i) (in case when the contact is formed between superconducting electrodes). Schematic presentation of contact is given in Fig. 1.4a.
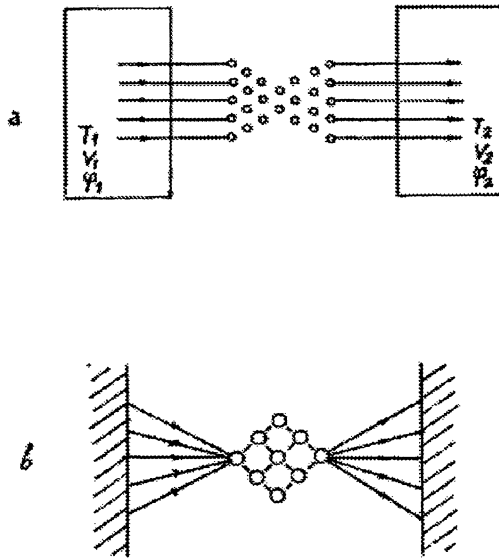

Figure 1.4 Models of the atomic contact with $N = 26$, $N_t = 2$, and $N_l = 5$ (*a*), and of the atomic link with $N = 9$, $N_l = 5$ (*b*).

Perfect contact geometry assumes that the number of leads, N_l, is much larger than the product of the number of the **transition channels** N_t to the number of **conduction channels** N_c. By the latter we mean, for example s, p_x, p_y, p_z, etc. electronic bands, or their hybridized bands. The channels are presented with their respective hopping amplitudes (transfer matrix elements) t_s and the positions of band centers ε_s, $s = 1, ..., N_c$. The Hamiltonian of the junction is

$$H = \sum_{s=1}^{N_c} \left(\varepsilon_s \sum_{i=1}^{N} c_{is}^+ c_{is} - t_s \sum_{<i,j>} c_{is}^+ c_{js} \right) + H_{lead} \qquad (1.8)$$

where

$$H_{lead} = -t \sum_{k=1}^{N_l} \left(\sum_{n=1}^{\infty} a_{nk}^+ a_{n+1,k} + \sum_{s=1}^{N_c} a_{1k}^+ c_{ks} \right) + \text{h.c.}$$

$$-t \sum_{k=1}^{N_l} \left(\sum_{n=1}^{\infty} b_{nk}^+ b_{n+1,k} + \sum_{s=1}^{N_c} b_{1k}^+ c_{N-k+1,s} \right) + \text{h.c.} \qquad (1.9)$$

The atoms in the central part of contact are numbered from 1 to N (the electron creation operators at atom sites are c_{is}^+, $i = 1, ..., N$, $s = 1, ..., N_c$ connected to the left and right leads with the creation operators a_{1k}^+, $k = 1, ..., N_l$, and b_{1k}^+, $k = N - N_l + 1, ..., N$, respectively). We assume that electrons arrive to the contact through the leads from the left reservoir independently from one another, and are transmitted to the right reservoir after passing the contact with the transit amplitudes $t_{ks,k's'}$. Then, according to Landauer [1] and Imry [20] the contact conductance at $T = 0$ may be expressed as

$$G = G_0 \sum_{k,k'=1}^{N_l} \sum_{s,s'=1}^{N_c} |t_{ks,k's'}|^2. \qquad (1.10)$$

Calculation shows the dependence of the conductance on the occupation level (the Fermi energy μ) in metals. Typical dependences $G(\mu)$ are presented in Figs. 1.5 and 1.6. They show that the conductance, although in its magnitude of the order of the conductance quantum, is not exactly equal to or multiple of G_0. The non-monotonic behavior of conductance versus energy is an inevitable consequence of the scattering concept, and follows as a result of quantum reflection at the contact boundary.

Maximal conductance is proportional to the number of conducting channels N_c and also to the number of contacting points (the "transition channels") N_t in the narrowest part of metallic connection

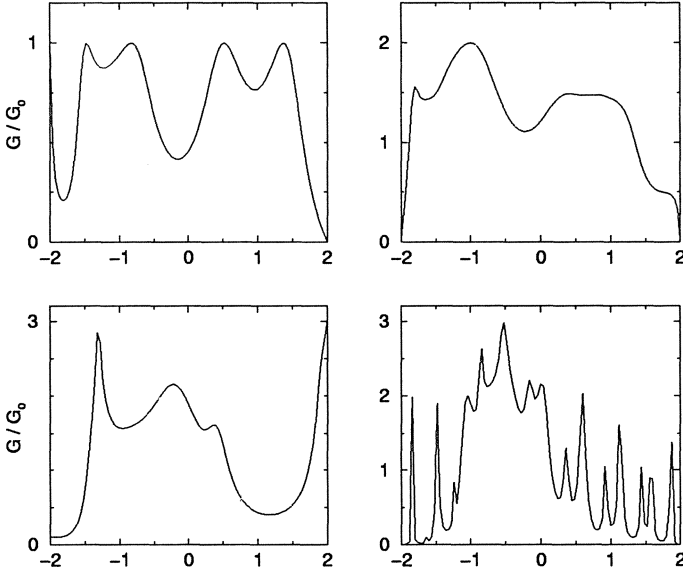$$G_{max} \leq N_c N_t G_0. \qquad (1.11)$$

Figure 1.5 Examples of the calculated conductance versus Fermi energy dependences in the atomic contacts with $t = t_s = -1$ and $\varepsilon_s = 0$. Upper left panel: 2d contact with $N_t = 1$, $N_c = 1$, $N_l = 5$, $N = 29$, $L = 0$. Upper right panel: 2d contact with $N_t = 2$, $N_c = 1$, $N_l = 5$, $N = 26$, $L = 0$. Lower left panel: 3d contact with $N_t = 3$, $N_c = 1$, $N_l = 30$, $N = 57$, $L = 0$. Lower right panel: 3d contact with $N_t = 3$, $N_c = 1$, $N_l = 30$, $N = 81$, and the channel between the tips of length $L = 8$.

Conductance is independent of the number of the "lead channels" N_l provided that N_l is larger than $N_c N_t$. These are the conclusions derived from the "rigid" model of the contact which assumes that the electron distribution in the contact area is not subject to variations due to proximity with the bulk electrodes. There is a reason, however, to believe that such variations may take effect.

Consider in particular the contact in the form of a link presented in Fig. 1.4b. Conductance $G(\mu)$ displays sharp peaks (Fig. 1.6) which correspond to the transmittance resonances at the discrete levels in the link. Similar resonances also appear in $G(U)$ dependence where U is the energy shift added to the atoms at the inner sites. If we allow for charge to accumulate in the link, or to deplete from the atoms in the inner block, the Fermi level in the link will level off with one of such resonances with the result that the transmissivity between the left and right electrodes substantially increases which in turn will lower the total system energy. The spontaneous accumulation (depletion) of charge at the link is therefore energetically favorable. We may assume that contact may automatically adjust its Fermi level by accreting (or losing)
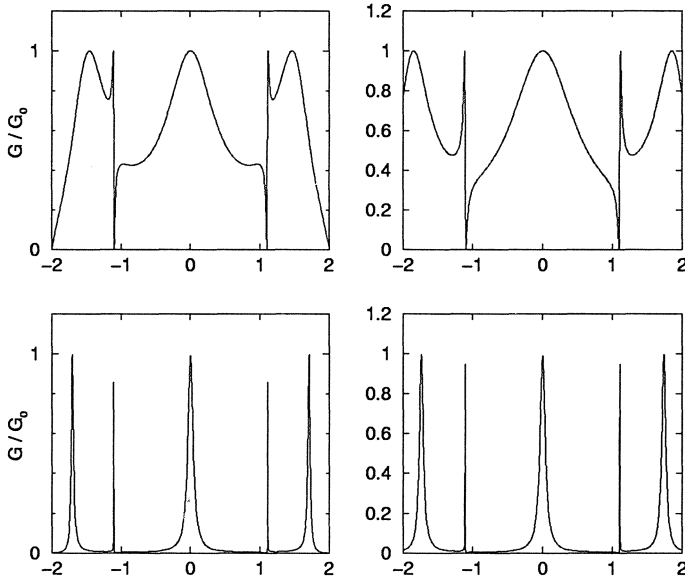
Figure 1.6 Conductance of atomic link with parameters $t = t_s = -1$, $N = 9$, $N_c = 1$ (see Fig. 1.4b). Upper panels correspond to $N_l = 3$ (left panel) and $N_l = 30$ (right panel), and show the dependence of conductance on the Fermi energy μ (in units of $|t|$). Lower panels correspond to same values of N_l, and show the dependence of conductance on the energy shift added to atoms in the link, U (in units of $|t|$) at $\mu = 0$.

some charge from bulk metals. Of course, this will cost some energy of charging the link, of the order of e^2/d, which however is less than the energy gain due to increased transmissivity (of order of t) provided that $d \gg a$ and assuming that $|t| \sim e^2/a$.

This is opposite to the Coulomb blockade situation [21] characteristic of weakly coupled granules to the banks ($|t| \ll e^2/a$) in which, because of small $|t|$, the metallic cohesion energy between the granule and the massive electrode is insignificant. We conclude therefore on the possibility of explaining the exact quantization of conductance in contacts which is often found in an experiment, in terms of the self-charging effect of atoms in constriction.

3. BALLISTIC MICROCONTACTS

Contacts with the size of the contact area d much larger than the interatomic spacing can be treated semiclassically by introducing the distribution of electrons in the momentum and coordinate space $f(\mathbf{p}, \mathbf{r})$ and solving for $f(\mathbf{p}, \mathbf{r})$ from the Boltzmann equation. Sharvin [2] as-
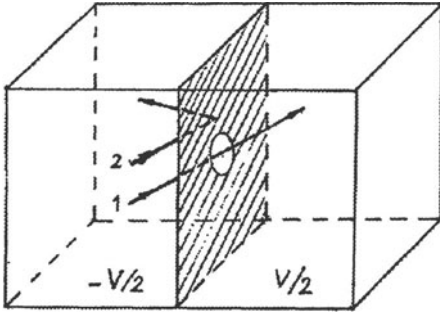
Figure 1.7 Sketch of contact in the form of an orifice in the nontransparent screen. 1) electron trajectory piercing through the orifice, 2) trajectory reflecting from the screen. At the fixed direction of the electron momentum **p**, probability of electron transition between the two boxes is equal to the ratio between surface of the orifice and the surface of screen.

sumed that contact conductance in this case is independent of the mean free path and may be estimated as

$$G \simeq \sigma \frac{d^2}{l} \sim \frac{ne^2 d^2}{p_F} \tag{1.12}$$

where σ is the bulk conductivity and l the mean free path of electron. Since product σl is independent of the mean free path, so the full conductance will be. The calculation of the Sharvin conductance can be achieved with the help of the Landauer formula (1.10), or by using directly the Boltzmann approach [13].

In the Landauer language, we may assume that the probability of electron traversing the impenetrable screen through the circular orifice of surface S in it (Fig. 1.7) is equal to the ratio of S to the total surface of the screen S_0,

$$T = |t|^2 = S/S_0 . \tag{1.13}$$

Summation over the states of electron in a box is semiclassically equivalent to integration over $dp_x dp_y$ with a factor $L_x L_y/(2\pi\hbar)^2$ where L_x, L_y are transverse dimensions of the quantization box, thus giving for the conductance

$$G = \frac{2e^2}{h} \frac{S}{S_0} \int_{p_x^2+p_y^2<p_F^2} \frac{L_x L_y dp_x dp_y}{(2\pi\hbar)^2} = \frac{2e^2}{h} N_\perp \tag{1.14}$$

where $N_\perp$ is defined as the number of transverse channels corresponding to the contact area S:

$$N_\perp = \frac{S k_F^2}{4\pi}. \tag{1.15}$$

This is the number of states at the Fermi energy per cross sectional area S. The expression (1.14) clearly complies with the Sharvin conductance (1.12). In the alternative derivation of contact conductance using the Boltzmann approach [13], we calculate the current at the orifice as

$$J = 2eS \int f(\mathbf{p}) v_z \frac{d^3 p}{(2\pi\hbar)^3} \tag{1.16}$$

where f is the distribution function at $z = 0$, by using the expression for the latter

$$f(\mathbf{p}) = f_0\left(\varepsilon_{\mathbf{p}} - \frac{eV}{2}\,\mathrm{sgn}v_z\right). \tag{1.17}$$

Such form is an immediate consequence of the energy conservation on the ballistic electron trajectory entering the orifice from the left box ($z = -\infty$) in case when the velocity of the electron at orifice is positive ($v_z > 0$), or from the right box ($z = +\infty$) if the velocity is negative ($v_z < 0$). f_0 is an equilibrium Fermi distribution $f_0(\varepsilon) = 1/[\exp{(\varepsilon - \mu)/T}+1]$, V is the voltage difference between metals. Left box and the right box are the two "thermal reservoirs" since at any point inside the box, except at the immediate vicinity of the contact ($|\mathbf{r}| \sim d$), distribution of electrons is the equilibrium one. The electrons with z-component of velocity $v_z > 0$ at $z = 0$ are in equilibrium at $z = -\infty$ where the maximal energy of Fermi distribution equals to $\varepsilon_F + eV/2$ whereas the electrons having z-component of velocity $v_z < 0$ at $z = 0$, arrive from $z = +\infty$ where the maximal energy is $\varepsilon_F - eV/2$. Expanding f in Eq. (1.16) in powers of eV/ε_F, we receive at $V \to 0$ the current at the orifice

$$J = -\frac{2eS}{h^3}\frac{eV}{2}\int\frac{\partial f_0}{\partial\varepsilon_p}|v_z|d^3p = GV \tag{1.18}$$

with the conductance

$$G = \frac{e^2SS_F}{2(2\pi\hbar)^3} \tag{1.19}$$

S_F is the surface of the Fermi sphere $4\pi p_F^2$. This formula is equivalent to the Landauer expression, Eq. (1.14).

According to the derivation presented, distribution of electrons at the orifice consists ot two electron "beams" moving in opposite directions with maximal energies at the truncated Fermi surface equal to $\varepsilon_F \pm eV/2$ (see Fig. 1.8a).

At any point $\mathbf{r}$ away from the orifice, the truncated Fermi surface has same energy shift between two parts, eV, but the parts are inequivalent in size. The electron distribution at point $\mathbf{r}$ equals to

$$f(\mathbf{p},\mathbf{r}) = f_0[\varepsilon_{\mathbf{p}} + e\phi(\mathbf{r})\,\mathrm{sgn}v_z] \tag{1.20}$$

where $\phi(\mathbf{r})$ is the electrostatic potential at point $\mathbf{r}$, and $\Omega(\mathbf{r})$ is a solid angle showing orifice from point $\mathbf{r}$. By requiring that charge density remains unchanged (the condition of the local neutrality) at any point $\mathbf{r}$, we find the potential distribution

$$\phi(\mathbf{r}) = \frac{V}{2}\left[1 - \frac{\Omega(\mathbf{r})}{4\pi}\right]\,\mathrm{sgn}z. \tag{1.21}$$
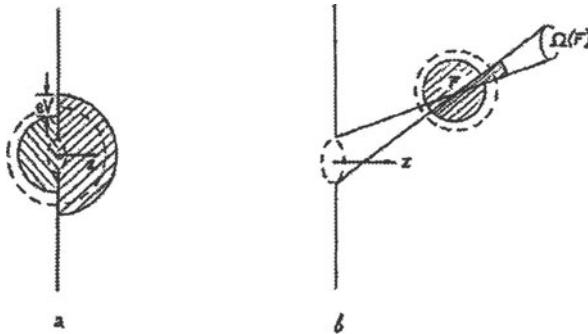
Figure 1.8 Distribution of electrons at the contact surface (*a*), and at point r outside the surface (*a*). $\Omega(\mathbf{r})$ is a solid angle at which the orifice is seen from r. Fermi surface at each point is truncated along the line which is an image of the orifice to the Fermi sphere. The energy difference between two parts of truncated Fermi surface equals at each point to eV.

which along z axis becomes

$$\phi(z) = \frac{V}{2} \frac{z}{\sqrt{z^2 + d^2/4}} \qquad (1.22)$$

The voltage continuously changes from $-V/2$ to $V/2$ at distances from the orifice of the order of its diameter d which is much smaller than the mean free path of electron l. Within the distances of order d near the orifice, a strongly nonequilibrium stationary state exists as long as a current is supplied through the contact. Since energy is conserved along the electron trajectory, Joule heat is not released inside the contact and is transferred to the lattice only at distances of order l much away from the orifice.

The Landauer calculation directly relates conductance G to the number of conducting channels inside the contact, $N_\perp$. It was then argued [22] that if the number of transverse channels changes discretely at the increasing contact diameter, so the conductance will do, *i.e.* G will be an integer multiple of the conductance quantum $2e^2/h$. It was assumed that in a smooth contact continuously changing its diameter from infinity to d in the narrowest part, discrete channels will open one by one thus resulting in a conductance quantization $G = nG_0$.

These considerations do not apply directly to the atomic contacts. Subsequent microscopic calculation of the waveguide modes in a finite-size contact of various geometry [23]-[26] showed oscillatory behavior (see Fig. 1.9) as a function of occupation, which however to our knowledge have been never observed. We suggest that the self-focusing behavior
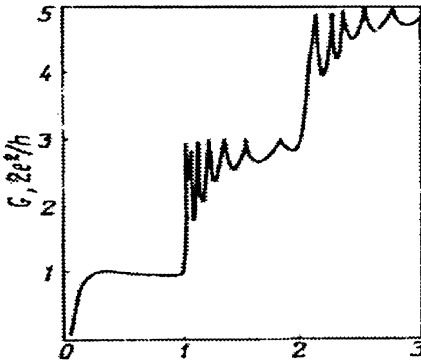
Figure 1.9 Conductance of ballistic contact in a form of cylinder of length L such that $k_F L = 40$, as a function of the parameter $k_F d/2$. Taken from Ref. [27].

of electron concentration near the contact "throat" discussed in page 9 may instead be relevant to the observed discrete G values.

4. INELASTIC SCATTERING AND J−V NONLINEARITY IN SEMICLASSICAL CONTACTS

According to Landauer or Boltzmann theory of ballistic contact conductance, its J−V dependence is linear up to biases of the order of Fermi energy. Introduction of the inelastic scattering of electrons on phonons results in the nonlinearity of the current-voltage characteristics at energy of the order of typical phonon energies [6]. This nonlinearity serves as a tool of the phonon spectroscopy in metals [3, 4, 28, 29, 30] since the nonlinear dependence is directly related to the density of phonon states at voltage bias equal to phonon energy,

$$eV = \hbar\omega. \tag{1.23}$$

To find the nonlinear correction to the contact current, we need to calculate $f_{\mathbf{p}}$ from the Boltzmann equation

$$\frac{\partial f_{\mathbf{p}}}{\partial t} + \frac{\partial \varepsilon_p}{\partial \mathbf{p}} \frac{\partial f_{\mathbf{p}}}{\partial \mathbf{r}} - e \frac{\partial \phi}{\partial \mathbf{r}} \frac{\partial f_{\mathbf{p}}}{\partial \mathbf{p}} = I_{e-ph}\{f_{\mathbf{p}}, N_{\mathbf{q}}\} \tag{1.24}$$

and to find the phonon distribution $N_{\mathbf{q}}$ from

$$\frac{\partial N_{\mathbf{q}}}{\partial t} + \frac{\partial \omega_{\mathbf{q}}}{\partial \mathbf{q}} \frac{\partial N_{\mathbf{q}}}{\partial \mathbf{r}} = I_{ph-e}(N_{\mathbf{q}}, f_{\mathbf{p}}) \tag{1.25}$$

where I_{e-ph} and I_{ph-e} are the electron-phonon and phonon-electron collision integrals

$$I_{e-ph} = \sum_{\mathbf{q}} W_{\mathbf{q}}\{[f_{p+q}(1 - f_p)(N_q + 1) - f_p(1 - f_{p+q})N_q]\delta(\varepsilon_{p+q} - \varepsilon_p - \omega_q)$$

$$+[f_{p-q}(1 - f_p)N_q - f_p(1 - f_{p-q})(N_q + 1)]\delta(\varepsilon_{p-q} - \varepsilon_p + \omega_q)\} \quad (1.26)$$

and

$$I_{ph-e} = 2W_{\mathbf{q}} \sum_{\mathbf{p}} [f_{p+q}(1 - f_p)(N_q + 1) - f_p(1 - f_{p+q})N_q]\delta(\varepsilon_{p+q} - \varepsilon_p - \omega_q)$$

$$(1.27)$$

$W_{\mathbf{q}} = (2\pi\hbar)|M_{\mathbf{q}}|^2$ where $M_{\mathbf{q}}$ is the matrix element of electron-phonon interaction.

To find the nonlinear correction to current, we solve Eqs. (1.24) and (1.25) to first order in the collision integral which are in effect the first corrections in the ballistic small parameters d/l_{e-ph} and d/l_{ph-e} where l_{e-ph} and l_{ph-e} are the electron-phonon and phonon-electron mean free paths, respectively. In the nonequilibrium state, the mean free paths are defined as

$$\frac{1}{l_{e-ph}(\varepsilon, T)} = \frac{2\pi}{v_F} \int_0^{\omega_m} (2N_\omega + 1 + f_{\varepsilon+\omega} - f_{\varepsilon-\omega})\alpha^2(\omega)F(\omega)d\omega \quad (1.28)$$

and

$$\frac{1}{l_{ph-e}(\omega, T)} = \frac{4\pi}{v_F} N(\varepsilon_F)\omega\alpha^2(\omega) \quad (1.29)$$

where $N(\varepsilon)$ and $F(\omega)$ are the electron and phonon densities of states, and $\alpha^2(\omega)$ is the square of the matrix element of electron-phonon interaction averaged over the Fermi surface. The product

$$g(\omega) = \alpha^2(\omega)F(\omega) \quad (1.30)$$

is known as a function of electron-phonon interaction (the Eliashberg function) and is defined as

$$g(\omega) = \frac{1}{(2\pi)^3} \int \frac{dS_p}{v_p} \frac{dS_{p'}}{v_p'} W_{\mathbf{p}-\mathbf{p'}}\delta(\omega - \omega_{\mathbf{p}-\mathbf{p'}}) / \int \frac{dS_p}{v_p} \quad (1.31)$$

(integration is running over the Fermi surface, $v_{\mathbf{p}} = |\partial\varepsilon_p/\partial\mathbf{p}|$ is electron velocity at $\varepsilon = \varepsilon_F$). At $T = 0$ and at energy equal to the Debye energy, mean free paths can be estimated as

$$l_{e-ph} \sim l_{ph-e} \sim \frac{v_F}{\lambda\omega_D} \quad (1.32)$$

where λ is a dimensionless electron-phonon coupling constant

$$\lambda = 2 \int_0^\infty g(\omega)\frac{d\omega}{\omega}. \quad (1.33)$$

Typically, $\lambda \sim 0.1-1$ in most metals, therefore both the electron-phonon and the phonon-electron mean free paths are of order of $10 - 100$ nm at

$\varepsilon \sim \hbar \omega_D$, whereas the electron-phonon and phonon-electron scattering frequencies differ by 3 order of magnitude:

$$\tau_{e-ph}^{-1} \sim 10^{13}\ \mathrm{s}^{-1}, \quad \tau_{ph-e}^{-1} \sim 10^{10}\ \mathrm{s}^{-1}. \tag{1.34}$$

Solving Eq. (1.24) perturbatively to first order in d/l_{e-ph}, we receive for the correction to the distribution function an expression

$$f_1 = e\phi_1 \frac{\partial f_0}{\partial \varepsilon_p} + \int_{-\infty}^{0} I_{e-ph}(\mathbf{p}(t), \mathbf{r}(t))dt \tag{1.35}$$

where ϕ_1 is a correction to the electrostatic potential. $\mathbf{p}(t)$ and $\mathbf{r}(t)$ are the momentum and the coordinate at electron trajectory at time t. At $eV \ll \varepsilon_F$, the trajectory is a straight line arriving at time $t = 0$ to point $\mathbf{r}$ from $-\infty$ or from $+\infty$ at $t = -\infty$, depending on the direction of the electron velocity $\mathbf{v}$. The potential can be found from the electroneutrality $< f_1 >= 0$. The first order correction to the current

$$J_1 = 2e \int dxdy \int \frac{d^3p}{h^3} v_z f_1(\mathbf{p}, \mathbf{r}). \tag{1.36}$$

is received finally in the form [6, 30]

$$J_1 = -\frac{2e\Omega_{eff}}{(2\pi)^6} \int_0^\infty d\omega L(\omega, eV, T) \int \frac{dS_p}{v_p} \int \frac{dS_{p'}}{v_p'} K(\mathbf{v}, \mathbf{v}') W_{\mathbf{p}-\mathbf{p}'} \delta(\omega - \omega_{\mathbf{p}-\mathbf{p}'}) \tag{1.37}$$

where

$$L(\omega, \varepsilon, T) = M(\omega, \varepsilon) - M(\omega, -\varepsilon), \quad M(\omega, \varepsilon) = \frac{(\omega - \varepsilon)(e^{\varepsilon/T} - 1)}{[1 - e^{(\varepsilon-\omega)/T}](e^{\omega/T} - 1)} \tag{1.38}$$

where $\Omega_{eff} = d^3/3$ is an effective volume near the orifice in which nonequilibrium phonons are emitted by "hot" electrons. Backscattering of electrons is the cause of such emission and serves to the decrease the of electron current.

At fixed phonon frequency, $J - V$ curve changes its slope at $eV = \hbar\omega$ (Fig. 1.10), while the second derivative of J with respect to V acquires a negative peak. For the continuous distribution of phonons on frequency, $F(\omega)$, the derivative of conductance with respect to voltage takes form

$$G^{-1}\frac{dG}{dV} = -\frac{8ed}{3\hbar v_F} \int_0^\infty g_c(\omega) \chi\left(\frac{\omega - eV}{T}\right) \frac{d\omega}{T} \tag{1.39}$$

at finite temperature T, and

$$G^{-1}\frac{dG}{dV} = -\frac{8ed}{3\hbar v_F} g_c(eV) \tag{1.40}$$
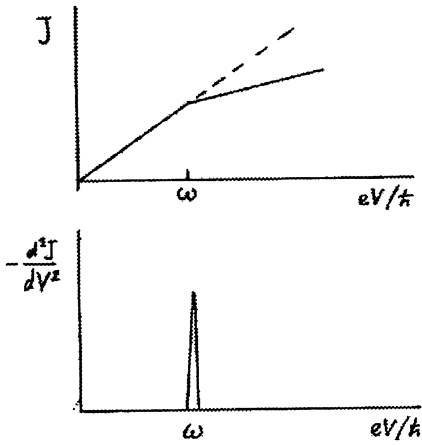
Figure 1.10 $J - V$ characteristics (a) and its second derivative (b) for a contact with fixed phonon frequency ω.
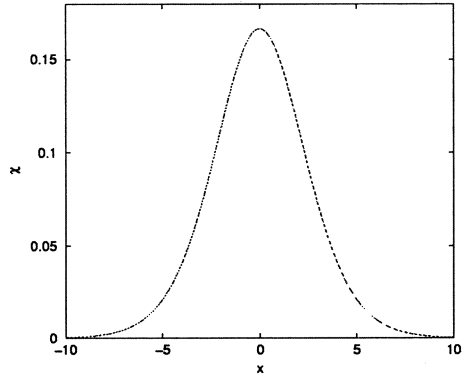
Figure 1.11 Temperature broadening of the phonon spectrum. The linewidth at the half height equals to 5.44.

at $T = 0$. $\chi(x)$ is the temperature broadening function (Fig. 1.11)

$$\chi(x) = \frac{d^2}{dx^2}\left(\frac{x}{e^x - 1}\right) \tag{1.41}$$

and $g_c(\omega)$ is the transport function of electron-phonon interaction

$$g_c(\omega) = \frac{1}{(2\pi)^3}\int\frac{dS_p}{v_p}\frac{dS_{p'}}{v'_p}K(\mathbf{v}, \mathbf{v}')W_{\mathbf{p}-\mathbf{p}'}\delta(\omega - \omega_{\mathbf{p}-\mathbf{p}'})/\int\frac{dS_p}{v_p} \tag{1.42}$$

which differs from the Eliashberg function (1.31) in a an additional form factor, the so called K-factor, $K(\mathbf{v}, \mathbf{v}')$, taking into consideration the kinematic restrictions on electron scattering at the orifice. In the case of circular orifice

$$K(\mathbf{v}, \mathbf{v}') = \frac{4|v_z v_{z'}|\theta(-v_z v_{z'})}{|v_z\mathbf{v}' - v'_z\mathbf{v}|}. \tag{1.43}$$

where $\theta(x)$ is a step function, $\theta(x) = 1$ at $x = 0$ and $\theta(x) = 0$ at $x < 0$.

The function $K(\mathbf{v}, \mathbf{v}')$ is singular at $\mathbf{v}' = -\mathbf{v}$ (for the reverse scattering) but since the singularity is an integrable one, it does not much affect the shape of $g_c(\omega)$ as compared to the isotropic EPI function $g(\omega)$ (mention that K in Eq. (1.43) is normalized to unity, $< K >_{FS} = 1$). For a spherical Fermi surface with the matrix element of EPI depending only on the transfer momentum $\mathbf{q} = \mathbf{p}' - \mathbf{p}$, the important is the dependence

of K on the scattering angle θ

$$q = |\mathbf{p}' - \mathbf{p}| = 2p_F \sin\frac{\theta}{2}, \tag{1.44}$$

and on the angle γ between the direction of $\mathbf{q}$ and the normal $\mathbf{n}$ to metal surface

$$\gamma = \arccos(\mathbf{q}, \mathbf{n}).$$

The integration over the other angles gives

$$K(\theta, \gamma) = \frac{2}{\pi \sin\theta} \int_{\varphi_0}^{\pi/2} \frac{\sin^2\frac{\theta}{2}\cos^2\gamma - \cos^2\frac{\theta}{2}\sin^2\gamma\cos^2\varphi}{(\cos^2\varphi + \cos^2\gamma\sin^2\varphi)^{1/2}} d\varphi \tag{1.45}$$

where $\varphi_0 = \arccos(\tan\frac{\theta}{2}/\tan\gamma)\theta(\gamma - \theta/2)$ (in Fig. 1.12 we present a 3*d* plot of $K(\theta, \gamma)$). Some authors (see [31]) further integrate K over γ to receive

$$\bar{K}(\theta) = \frac{1}{2}\left(1 - \frac{\theta}{\tan\theta}\right). \tag{1.46}$$

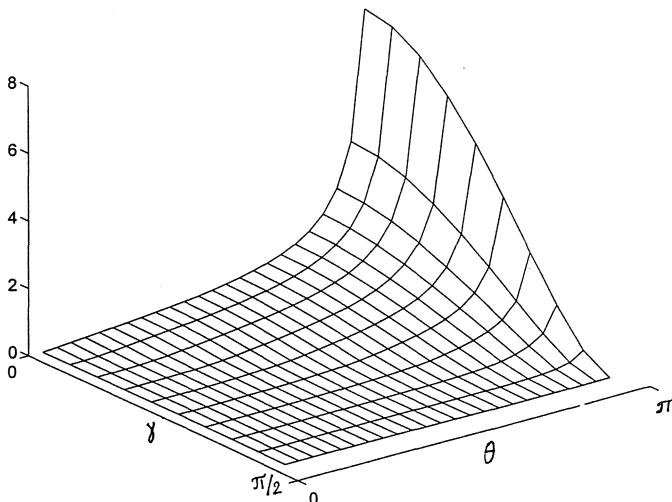The singularity mentioned above is at $\theta = \pi$.

Figure 1.12   3*d* plot of K-factor $K(\theta, \gamma)$ in a circular orifice.

The above results have been generalized to the models of contact of various geometry (the orifice, the channel, *etc.*) [32] and to scattering conditions concerning elastic (impurity) scattering [33]. Such scattering in itself does not lead to the nonlinearity of the $J(V)$ but decreases the

phonon nonlinear part of d^2J/dV^2 as compared to the perfect ballistic regime. In a **diffusive** contact,

$$l_i \ll d \ll l_{ph-e}, \tag{1.47}$$

scattering by phonons can be calculated as an effect proportional to $(l_id)^{1/2}/l_{e-ph}$, where l_i is the elastic (impurity) scattering length of electron. The nonlinear part of $J(V)$ can in a diffusive contact be presented in the same form as in a ballistic contact, with an appropriate K-factor. In Table. 1.1, K-factors are listed for some contact geometries.

Table 1.1 K-factors of contacts with various geometries. d is the diameter of the orifice or cylindrical channel, L is the length of the channel. n is a unit vector in the direction of electron velocity v, l_i is the elastic mean free path of electron, l_ε is the inelastic (electron-phonon) mean free path.

Contact geometry	K-factor	Parameters
Orifice in clean metal	$4\|n_z n_z'\|\theta(-n_z n_z')/\|n_z \mathbf{n}'- n_z'\mathbf{n}\|$	$d \ll l_i$
Orifice in dirty metal	$3[(\mathbf{n}_\perp - \mathbf{n}'_\perp)^2 + 2(n_z - n_z')^2]/8$	$l_i \ll d \ll \sqrt{l_i l_\varepsilon}$
Clean channel	$2\theta(-n_z n_z')$	$L \gg d$
Dirty channel	$3(n_z - n_z')^2/2$	$d, l_i \ll L \ll \sqrt{l_i l_\varepsilon}$

Another example of inelastic scattering is associated with the localized lattice defects, the so called two-level systems (TLS) [34, 35]. The general treatment of inelastic scattering by TLS is similar to that of phonons, except that the population of TLS is strongly eV- dependent and in itself contribute to the lineshape of the point-contact spectrum. Fig. 1.1 shows this nonsymmetric lineshape of the TLS's point-contact spectra at various temperatures.
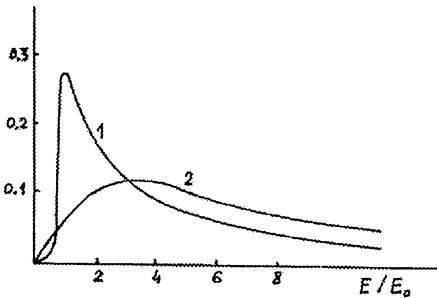

Figure 1.13 Two-level-system point-contact spectrum lineshape at $T/E_0 = 0.1$ (line 1) and at $T/E_0 = 0.5$ (line 2). Taken from Ref. [34].

5. PHONON TRAPPING AND RELAXATION

Inelastic events of electron-phonon interaction result in the phonon emission from the narrowest part of the contact. Since the phonon mean free path is much larger than the contact dimension, the phonons leave the contact and release their energy away from the nonequilibrium part of the junction. In plastically deformed constrictions, however, phonons can be scattered back and reabsorbed near the orifice. The nonequilibrium phonon gas with an effective temperature T^* much larger than the ambient temperature T is then formed near the region of nonequilibrium electrons.

The nonequilibrium phonons increase the electron scattering near the orifice and produce an additional nonlinearity in the $J-V$ curve, in particular the nonzero value of d^2J/dV^2 at voltage larger than the maximal phonon energy. Such *background* point-contact spectroscopy signals are often observed in microcontacts of the needle-anvil geometry [36].

The second derivative of the $J-V$ characteristics of microcontact in the phonon reabsorption regime can be presented in the form [15]

$$G^{-1}\frac{dG}{dV} = -\frac{8ed}{3\hbar v_F}[g_c(eV) + B(eV)] \qquad (1.48)$$

where the background part, $B(eV)$, is presented as

$$B(\varepsilon) = 2\frac{d^2}{d\varepsilon^2}\left\{\varepsilon\int_0^\infty \frac{g(\omega)d\omega}{e^{\omega/T^*} - 1}\right\}. \qquad (1.49)$$

The effective temperature of the nonequilibrium phonons T^* is found from the equation of energy balance

$$\int_0^{eV}(eV - \omega)\tilde{g}(\omega)\omega d\omega = 2\int_0^\infty \frac{g(\omega)\omega^2 d\omega}{e^{\omega/T^*} - 1} \qquad (1.50)$$

in which the function $\tilde{g}(\omega)$ differs from the conventional contact EPI function $g(\omega)$ with an additional factor $\theta(-p_z p_z')$ corresponding to integration over the half of the Fermi sphere. As an approximation, we assume then that $\tilde{g}(\omega) \sim (1/2)g(\omega)$. By introducing a factor η such that

$$\int_0^{eV}(eV - \omega)\tilde{g}(\omega)\omega d\omega = \eta\int_0^\infty \frac{g(\omega)\omega^2 d\omega}{e^{\omega/T^*} - 1} \qquad (1.51)$$

we receive

$$T^* \sim eV/\eta \qquad (1.52)$$

with $\eta \sim 4$. At the bias energy eV much above the phonon spectrum,
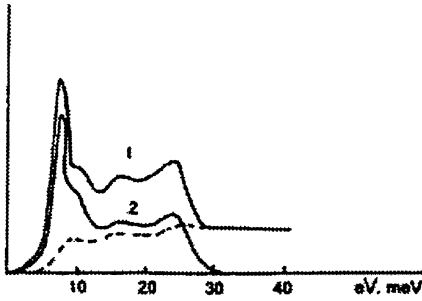
Figure 1.14 Point-contact spectrum of Zn contact [35] (line 1) decomposed into its spectral part (line 2) and to the background contribution (dashed line) [14].

$eV \gg \hbar\omega_D$, Eq. (1.49) gives

$$B(\infty) = \frac{4}{\eta} \int_0^\infty g(\omega) \frac{d\omega}{\omega} = \frac{2\lambda}{\eta}. \tag{1.53}$$

λ is the EPI coupling parameter, Eq. (1.33).

The Fig. 1.14 shows, as an example, the point contact spectrum (the derivative $-G^{-1}dG/dV(V)$) of a dirty Zn contact with a relatively large background [37], together with the EPI interaction function $g_c(\omega)$ received by inverting the integral equation (1.48). The latter have the unexpected property, namely, the strong frequency dependence with respect to frequency of current modulation used in the PC spectroscopy measurements [28]. The origin of frequency dependence is related to relaxation of nonequilibrium phonons. Trapped phonons have relaxation frequency of the order of the phonon-electron relaxation rate $\nu_{ph} \sim \tau_{ph-e}^{-1} \sim 10^{10}s^{-1}$. Trapping and desorbing of phonons is a relatively slow process as compared to the characteristic electron-phonon relaxation frequencies $\nu_{e-ph} \sim 10^{13}s^{-1}$.

Inelastic part of the current with trapped phonons is presented as

$$J_1(V) = \frac{8ed}{3\hbar v_F} G(0) \int_0^\infty d\omega\, g(\omega) \left[\frac{\omega + eV}{e^{(\omega+eV)/T} - 1} - \frac{\omega - eV}{e^{(\omega-eV)/T} - 1} - 2eVN(\omega) \right] \tag{1.54}$$

where the last term takes into account the effect of trapped phonons. At zero ambient temperature, the phonon distribution takes the simple form

$$N_\omega = \frac{eV - \omega}{\eta(\omega + \omega_0)} \theta(eV - \omega) \tag{1.55}$$

where ω_0 is the phonon escape frequency introduced in [15]. The last term in Eq. (1.54) (a PC background) is shown to depend on frequency of the external signal applied to the contact, $V = V_0 + V_1 \cos \omega t$, as

$$<J_1> = -\frac{2e^2 V_1^2 \eta}{\hbar v_F} G(0) \int_0^\infty g(\nu) \frac{\tau_{ph-e}^{-2}(\nu)}{\tau_{ph-e}^{-2}(\nu) + \omega^2} \frac{d\nu}{\nu} \tag{1.56}$$
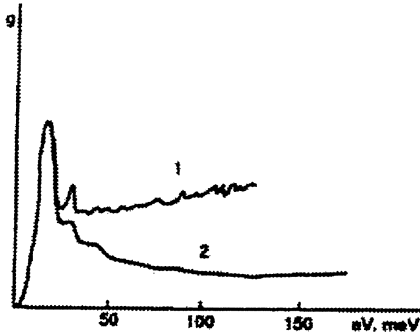
and shows the decrease above the cutoff ω_c of the order of the phonon-electron relaxation rate ν_{ph-e} [16] (Fig. 1.15).

6. THERMAL CONTACTS AND HOT SPOTS

In a thermal contact, electron and phonon mean free paths are smaller than the contact diameter d. Therefore, the lattice and electrons stay in equilibrium between themselves, but the temperature of this local equilibrium $T(\mathbf{r})$ is much higher than the ambient temperature of the environment. The distributions of temperature and electrostatic potential $\phi(\mathbf{r})$ are found from the equation of the energy balance

$$-\text{div}\mathbf{q} + \mathbf{jE} = 0, \quad \mathbf{q} = -\kappa\nabla T, \quad \mathbf{j} = \sigma\mathbf{E} \qquad (1.57)$$

where the local thermal conductivity $\kappa = \kappa(T(\mathbf{r}))$ and electrical conductivity $\sigma = \sigma(T(\mathbf{r}))$. Equations (1.57) are solved in a circular orifice with transformation to the oblate spheroidal coordinates $(a = d/2)$

$$\begin{aligned} x &= a\sin u\cosh v\cos\varphi \\ y &= a\sin u\cosh v\sin\varphi \\ z &= a\cos u\sinh v\,. \end{aligned} \qquad (1.58)$$

Eqs. (1.57) reduce to

$$\text{div}(\sigma\nabla\phi) = 0, \quad \frac{\pi^2 k_B^2}{6e^2}\text{div}[\sigma\nabla(T^2)] + \sigma(\nabla\phi)^2 = 0. \qquad (1.59)$$

Assuming further the applicability of the Wiedemann-Franz law relating κ to σ,

$$\frac{\kappa}{\sigma T} = \frac{\pi^2 k_B^2}{3e^2} \qquad (1.60)$$

and solving Eq. (1.59) in spheroidal coordinates, we receive potential and temperature distributions with no adjustable parameters

$$\phi(\mathbf{r}) = \frac{V}{2}\left(-1 + \frac{4}{\pi}\arctan e^v\right), \qquad (1.61)$$

$$T(\mathbf{r}) = \frac{eV\sqrt{3}}{2\pi}\left[1 - \left(1 - \frac{4}{\pi}\arctan e^v\right)^2\right]^{1/2} \qquad (1.62)$$

The temperature T_0 at the contact center, $v = 0$, is related to the applied voltage according to formula

$$eV = \frac{2\pi}{\sqrt{3}}k_B T_0 = 3.63\ k_B T_0 \qquad (1.63)$$

and is very much larger than the temperature in bulk.

Current-voltage relationship is strongly nonlinear and takes universal form

$$J(V) = G(0)V\int_0^1 \sigma_{red}\left(\frac{eV\sqrt{3}}{2\pi}\sqrt{1-x^2}\right)dx \qquad (1.64)$$

where $G(0)$ is a linear conductance $G(V \to 0)$ and $\sigma_{red}(T)$ is the reduced conductivity $\sigma_{red}(T) = \sigma(T)/\sigma(0)$. The current-carrying state in the thermal contact is of some interest, in particular with respect to possible application as a fast nonlinear switch or transistor [18, 38].

References

[1] R. Landauer, Electrical resistance of disordered one-dimensional lattices, Phil. Mag. **21**, 863 (1970).

[2] Yu. V. Sharvin, Possible method of Fermi surface investigation. Sov. Phys. JETP **21**, 655 (1965).

[3] I. K. Yanson, Nonlinear effects in the electrical conductance of point contacts and electron-phonon interaction in normal metals, Zh. Eksp. Teor. Fiz. **66**, 1035 (1974) [Sov. Phys. JETP **39**, 506 (1974)].

[4] A. G. M. Jansen, A. P. Van Gelder, and P. Wyder. Point-contact spectroscopy in metals. Journ. Phys. **F13**, 6073 (1980).

[5] B. J. Van Wees, H. Van Houten, C. W. J. Beenakker, J. G. Williamson, L. P. Kouwenhowen, D. Van Der Marel, and C. T. Foxon. Quantized conductance of point contacts in a two-dimensional electron gas. Phys. Rev. Lett. **60**, 848 (1988).

[6] I. O. Kulik, A. N. Omelyanchouk and R. I. Shekhter, Electrical conductivity of point microbridges and phonon and impurity spectroscopy in normal metals, Fiz. Nizk. Temp. **3** 1543 (1977) [Sov. J. Low Temp. Phys. **3**, 740 (1977)]; I. O. Kulik, R. I. Shekhter and A. N. Omelyanchouk, Electron-phonon coupling and phonon generation in normal metal microbridges, Sol. St. Commun., **23**, 301 (1977).

[7] J. M. Krans, J. M. Van Ruitenbeek, V. V. Fisun, I. K. Yanson and L. J. De Jongh, The signature of conductance quantization in metallic point contacts, Nature **375**, 767 (1995).

[8] I. O. Kulik and A. N. Omelyanchouk, Nonequilibrium fluctuations in normal-metal point contacts, Fiz. Nizk. Temp. **10** 305 (1984) [Sov. J. Low Temp. Phys. **10**, 158 (1984)].

[9] A. I. Akimenko, A. B. Verkin, and I. K. Yanson. Point-contact noise spectroscopy of phonons in metals. J. Low Temp. Phys. **54**, 247 (1984).

[10] M. J. M. De Jong, and C. W. J. Beenakker. Shot noise in mesoscopic systems, in: Mesoscopic Electron Transport, p.225. Eds. L. P. Sohn, L. P. Kouwenhowen, and G. Schoen. Kluwer, 1997.

[11] I. O. Kulik, Macroscopic quantization and the proximity effect in SNS junctions, Zh. Eksp. Teor. Fiz. **57**, 1745 (1969) [Sov. Phys. JETP **30**, 944 (1969)].

[12] I. O. Kulik, and A. N. Omelyanchouk, Contribution to the microscopic theory of the Josephson effect in superconducting bridges, Zh. Eksp. Teor. Fiz. Pis'ma **21**, 216 (1975) [JETP Lett. **21**, 96 (1975)]; I. O. Kulik and A. N. Omelyanchouk, Properties of superconducting microbridges in the pure limit, Fiz. Nizk. Temp. **3** 945 (1977) [Sov. J. Low Temp. Phys. **3**, 459 (1978)].

[13] A. N. Omelyanchouk, I. O. Kulik, R. I. Shekhter. Contribution to the theory of nonlinear effects in the electric conductivity of metallic junctions. JETP Lett, **35**, 437 (1977).

[14] Yu. G. Naydiuk, I. K. Yanson, A. A. Lysykh, O. I. Shklyarevskii. Electron-phonon interaction in microcontacts of Au and Ag, Fiz. Nizk. Temp. **8**, 922 (1982).

[15] I. O. Kulik, Nonequilibrium current-carrying states in metallic point contacts, Fiz. Nizk. Temp. **11** 937 (1985) [Sov. J. Low Temp. Phys. **11**, 516 (1985)].

[16] I. K. Yanson, O. P. Balkashin and Yu. A. Pilipenko, Relaxation of nonequilibrium phonons in metallic point contacts, Zh. Eksp. Teor. Fiz. Pis'ma **41**, 304 (1985) [JETP Lett. **41**, 372 (1985)].

[17] B. I. Verkin, I. K. Yanson, I. O. Kulik, O. I. Shklyarevskii, A. A. Lysykh, and Yu. G. Naydyuk. Singularities in d^2V/dI^2 dependences of point contacts between ferromagnetic metals. Sol. St. Commun. **30**, 215 (1979); I. O. Kulik. On the determination of $\alpha^2 F(\omega)$ in metals by measuring $I - V$ characteristics of "wide" (non-ballistic) point-contact spectra. Phys. Lett. **106A**, 187 (1984).

[18] I. O. Kulik. Nonlinear four-terminal microstructures: A hot-spot transistor. J. Appl. Phys. **76**, 1920 (1994).

[19] J. C. Cuevas, A. Levy Yeyati, and A. Martin-Rodero. Microscopic origin of the conducting channels in metallic atomic-size contacts. Phys. Rev. Lett. **80**, 1066 (1998).

[20] Y. Imry. Physics of mesoscopic systems, in: Directions in Condensed Matter Physics, p.101. Eds. G. Grinstein and G. Mazenko. World Scientific, Singapore, 1986.

[21] I. O. Kulik and R. I. Shekhter, Kinetic phenomena and charge discretness effects in granulated media, Zh. Eksp. Teor. Fiz. **68**, 623 (1975) [Sov. Phys. JETP **41**, 308 (1975)].

[22] L. I. Glazman, G. B. Lesovik, D. E. Khmelnitskii, and R. I. Shekhter. Reflection-free quantum transport and the fundamental jumps of ballistic resistance in microconstrictions. JETP Lett. **48**, 238 (1988).

[23] A. Szafer, and A. D. Stone. Theory of quantum conduction through a constriction. Phys. Rev. Lett. **60**, 300 (1989).

[24] E. Tekman, and S. Ciraci. Theoretical study of transport through a quantum point contact. Phys. Rev. **B43**, 7145 (1991).

[25] A. G. Scherbakov, E. N. Bogachek, and U. Landman. Quantum electronic transport through three-dimensional microconstrictions with variable shapes. Phys. Rev. **B53**, 4054 (1996).

[26] E. N. Bogachek, A. M. Zagoskin and I. O. Kulik, Conductance jumps and magnetic flux quantization in ballistic point contacts, Fiz. Nizk. Temp. **16** 1404 (1990) [Sov. J. Low Temp. Phys. **16**, 796 (1990)].

[27] A. M. Zagoskin, and I. O. Kulik. Quantum oscillations of the electrical conductivity of two-dimensional ballistic contacts. Sov. J. Low Temp. Phys. **16**, 911 (1990).

[28] I.K. Yanson, and A. V. Khotkevich. Atlas of Point Contact Spectra of Electron- phonon Interaction in Metals (in Russian), Naukova Dumka, Kiev, 1986; Engl. transl.: Kluwer Acad. Publ., 1995.

[29] A. M. Duif, A. G. M.Jansen, and P. Wyder. Point-contact spectroscopy. J. Phys. **C1**, 3157 (1989).

[30] I. O. Kulik, Ballistic and non-ballistic regimes in point-contact spectroscopy, Fiz. Nizk. Temp. **18** 450 (1992) [Sov. J. Low Temp. Phys. **18**, 302 (1992)].

[31] A. P. Van Gelder, On the structure of the d^2I/dV^2 characteristics of point contacts between metals, Sol. St. Commun. **35**, 19 (1980).

[32] M. Ashraf, and J. C. Swihart, Calculated point contact spectra of sodium and potassium, Phys. Rev. B25, 2049 (1982).

[33] I. O. Kulik, R. I. Shekhter and A. G. Shkorbatov, Point-contact spectroscopy of electron-phonon coupling in metals with a small electron mean free path, Zh. Eksp. Teor. Fiz. **81**, 2126 (1981) [Sov. Phys. JETP **54**, 1130 (1981)].

[34] V. I. Kozub, and I. O. Kulik, Microcontact spectroscopy of population of two-level systems, Zh. Eksp. Teor. Fiz. **91**, 2243 (1981) [Sov. Phys. JETP **64**, 1332 (1986)].

[35] R. J. P. Keijsers, O. I. Shklyarevskii, and H. Van Kempen, Point-contact study of fast and slow two-level fluctuators in metallic glasses, Phys. Rev. Lett. **77**, 3411 (1996).

[36] I. K. Yanson, I. O. Kulik, A. G. Batrak, Point-contact spectroscopy of electron-phonon interaction in normal metal single crystals, J. Low Temp. **42**, 527 (1981).

[37] I. K. Yanson, Point-contact spectroscopy of electron-phonon interaction in Zn and Cd, Fiz. Nizk. Temp. **3** 1516 (1977) [Sov. J. Low Temp. Phys. **3**, 726 (1977)].

[38] R. Ellialtıoğlu and İ. İ. Kaya, Conductance in metallic submicron cross-junctions, Chapter 33 of this volume, p. 479.